ResearchGate

See discussions, stats, and author profiles for this publication at:
https://www.researchgate.net/publication/229092264

Thiazyl chloride: An experimental and theoretical study of the valence shell HeI photoelectron spectrum

ARTICLE *in* CHEMICAL PHYSICS · FEBRUARY 2003

Impact Factor: 1.65 · DOI: 10.1016/S0301-0104(02)00966-7

CITATIONS
2

READS
35

9 AUTHORS, INCLUDING:

Denis Duflot
Université des Sciences et Technologi…
71 PUBLICATIONS **434** CITATIONS
SEE PROFILE

Jean-Pierre Flament
Université des Sciences et Technologi…
134 PUBLICATIONS **1,835** CITATIONS
SEE PROFILE

Alexandre Giuliani
SOLEIL synchrotron
100 PUBLICATIONS **971** CITATIONS
SEE PROFILE

Jacques Delwiche
University of Liège
119 PUBLICATIONS **1,538** CITATIONS
SEE PROFILE

Available from: Alexandre Giuliani
Retrieved on: 27 January 2016

Available online at www.sciencedirect.com
SCIENCE DIRECT®
Chemical Physics 288 (2003) 95–104
Chemical Physics
www.elsevier.com/locate/chemphys

Thiazyl chloride: an experimental and theoretical study of the valence shell HeI photoelectron spectrum

D. Duflot[a], N. Chabert[a], J.-P. Flament[a], J.-M. Robbe[a], I.C. Walker[b], J.H. Cameron[b], A. Giuliani[c], M.-J. Hubin-Franskin[c], J. Delwiche[d,*]

[a] *Laboratoire de Physique des Lasers, Atomes et Molécules (PhLAM), UMR CNRS 8523, Centre d'Études et de Recherches Lasers et Applications (CERLA), Université des Sciences et Technologies de Lille, F-59655 Villeneuve d'Ascq Cedex, France*

[b] *Department of Chemistry, Heriot-Watt University, Riccarton, Edinburgh EH14 4AS, UK*

[c] *Laboratoire de Spectroscopie d'Électrons Diffusés, Département de Chimie, Institut de Chimie B6c, Université de Liège, Sart Tilman, B4000 Liège 1, Belgium*

[d] *Thermodynamique et Spectroscopie, Département de Chimie, Institut de Chimie B6c, Université de Liège, Sart Tilman, B4000 Liège 1, Belgium*

Received 8 March 2002; in final form 21 October 2002

Abstract

High level (CASSCF-MRCI) ab initio calculations are used to investigate the structural, electronic and vibrational properties of the electronic ground state of thiazyl chloride (NSCl) and of the low-lying electronic states of $NSCl^+$. A new high resolution HeI photoelectron spectrum of NSCl has been recorded in the 10–16 eV energy region. From the results of the calculations, the first band is assigned to the $(1)^2A'$ state of $NSCl^+$. The second one corresponds to the $(2)^2A'$ and $(1)^2A''$ states which are quasi-degenerate. Despite the high resolution, the two first bands show no vibrational fine structure. For the first one, Franck–Condon analysis shows that it is due to the overlapping of two vibrational progressions involving the S–Cl stretching and the NSCl bending modes. In the case of the second band, it is explained by the highly repulsive character of the potential energy surfaces of two states of $NSCl^+$ in the Franck–Condon region of the neutral molecule. For the third band, which shows vibrational peaks, the calculation of Franck–Condon factors permits the determination of the adiabatic ionisation energy of the $(3)^2A'$ electronic state of $NSCl^+$ at 13.798 eV. Finally, the fourth band, which is due to three different ionic states with vibrational progressions, is too complicated to be assigned quantitatively.
© 2003 Published by Elsevier Science B.V.

PACS: 31.14.Ar; 33.60.Cv; 33.20.Tp

1. Introduction

Thiazyl chloride is the S-analogue of nitrosyl chloride, NOCl. At room temperature, it exists as a solid trimer, $N_3S_3Cl_3$, in equilibrium with the

* Corresponding author. Tel.: +32-4-3663435; fax: +32-4-3662941.
E-mail address: jdelwiche@ulg.ac.be (J. Delwiche).

0301-0104/03/$ - see front matter © 2003 Published by Elsevier Science B.V.
doi:10.1016/S0301-0104(02)00966-7

gaseous monomer. The trimer is a six-membered $(NS)_3$ ring having all the chlorine atoms on the same side of the ring. The monomer, characterised by both microwave spectroscopy [1] and electron diffraction [2], is a bent molecule (point group C_s) whose geometry is given in Table 1. Its infrared spectrum is known [3] (Table 2). Consistent with the tabulated data, the S–Cl bond is relatively weak (shared electron number = 0.60, compared with 2.14 for the N–S bond [4]) and photolysis of NSCl in the near UV generates a chlorine atom and an NS radical. However, there is little available information on the electronic states of NSCl. The HeI photoelectron spectrum (PES) was first reported by Cowan et al. [5] some years ago. It showed four unstructured bands between about 10.5 and 15 eV ionisation energy. These were assigned to five ionisations from comparison with the PES of thiazyl fluoride (NSF) together with the results of semi-empirical extended Hückel type calculations. Subsequently, De Kock et al. [6] published HeI and HeII spectra along with a NeI spectrum. In the last, the third and fourth ionisation bands showed fine structure suggesting excitation of the bend vibration, ν_2 (band 3) and the ν_1 stretch vibration (band 4) but the data were complicated by the doublet nature of the NeI source. A fifth ionisation was also reported. Cationic states were assigned using relative intensity differences between the HeI and HeII spectra and CNDO/2 calculations. Like Cowan et al., De Kock et al. [6] proposed two closely spaced ionisations within the second band, as did Allaf et al. from ab initio computations [7]. All of the above workers concur that the first cationic state is $^2A'$ followed by $^2A''$–$^2A'$ but thereafter, the state ordering is confused. It should be noticed that all previous theoretical studies applied Koopmans' theorem to assign the experimental bands.

As part of an investigation into the electronic structure of NSCl, we have carried out a high level ab initio theoretical study of the neutral ground state molecule and its low-lying cationic states, $NSCl^+$. We have also re-measured the HeI photoelectron spectrum, with energy resolution superior to that previously obtained; the spectrum is analysed using the results of the computations.

Table 1
Equilibrium geometries of the electronic ground state of $\tilde{X}^1A'$ of NSCl, at different levels of calculations

	RHF	RHF	CASSCF	CASSCF	CASSCF MRCI	CASSCF MRCI(D)	CASSCF MRCI(D)	RHF[a]	CPF[a]	CPF[a]	Exp.[b]	Exp.[c]
	cc-pVTZ	cc-pVQZ	cc-pVTZ	cc-pVQZ	cc-pVTZ	cc-pVTZ	cc-pVQZ	TZ + 2P	TZ + 2P	TZ + 3P	MW	X-ray
R_{NS} (Å)	1.432	1.425	1.468	1.461	1.470	1.464	1.455	1.444	1.488	1.487	1.450 ± 0.0001	1.448 ± 0.003
R_{SCl} (Å)	2.128	2.121	2.239	2.229	2.203	2.194	2.176	2.140	2.190	2.168	2.161 ± 0.0001	2.159 ± 0.003
$\theta_{(NSCl)}$ (°)	114.47	114.77	117.31	117.48	117.48	117.34	117.45	114.4	(117.7)	(117.7)	117.42 ± 0.05	117.5 ± 1.0

[a] Ref. [4].
[b] Ref. [1].
[c] Ref. [2].

Table 2
Vibrational wavenumbers[a] (cm^{-1}) of the electronic ground state $\tilde{X}^1A'$ of NSCl

	RHF cc-pVTZ	RHF cc-pVQZ	CASSCF cc-pVTZ	CASSCF cc-pVQZ	CASSCF MRCI cc-pVTZ	CASSCF MRCI(D) cc-pVTZ	CASSCF MRCI(D) cc-pVQZ	Exp.[b]	Exp.[c]	Exp.[d]
ω_1 (stretch NS)	1415.8	1429.0	1323.8	1332.4	1313.9	1351.9	1364.7			
ω_2 (bend NSCl)	314.0	318.5	267.1	268.1	272.1	276.8	281.3			
ω_3 (stretch SCl)	472.0	471.1	391.7	396.5	416.3	422.1	424.8			
ZPE	1101.8	1109.3	991.3	998.5	1001.2	1025.4	1035.4			
v_1 (stretch NS)	1394.7	1406.9	1308.4	1315.9	1297.6	1335.2	1351.9	1324.5 ± 1	1327.3	1326
v_2 (bend NSCl)	313.9	317.8	267.2	265.0	271.9	272.7	281.5	271.6 ± 1	267.4	
v_3 (stretch SCl)	470.6	464.6	379.1	400.6	405.1	422.3	431.6	414.8 ± 1	403.75	414
ZPE	1099.0	1094.7	987.8	990.8	997.1	1022.0	1035.1	1005.4	999.2	

[a] ω_1, ω_2, and ω_3 correspond to the harmonic vibrations, while v_1, v_2, and v_3 correspond to the anharmonic vibrations.
[b] Ref. [3].
[c] Ref. [27].
[d] Ref. [7].

2. Computational details

All the ab initio calculations in this paper were carried out with the MOLPRO program package [8]. Two Gaussian atomic orbital basis sets, taken from Dunning [9], were used: the cc-pVTZ (98 basis functions) and the cc-pVQZ (173 basis functions) basis sets.

The molecular orbitals (MOs) were optimised at the RHF and CASSCF [10–12] levels. In the latter case, the active space consists of the $n = 2$ shell for the N atom and the $n = 3$ shell for the S and Cl atoms, the inner shells being kept inactive. Thus, for the $\tilde{X}^1A'$ ground state of NSCl, the active space consists in 9 a′ MOs, 3 a″ MOs with 18 active electrons, leading to 8029 CSFs. For $NSCl^+$, there are 17 active electrons and the size of the active spaces are much larger (28,503 CSFs for $^2A'$ states and 28,125 CSFs for $^2A''$ states). In order to take into account the effect of dynamical correlation, multi-reference configuration interaction (MRCI) [13,14] calculations were performed, using the CASSCF MOs as starting orbitals. We recall that this method generates *all* single (S) and double (D) excitations from the configurations state functions (CSFs) of the active space. This leads to CI dimensions too large for our present computational possibilities, especially for $NSCl^+$. For example the MRCI space for the $^2A'$ states of $NSCl^+$ contains about 3×10^9 CSFs. To reduce the size of the calculations, the standard method is to generate the excitations from a sub-space of the active space, consisting of the CSFs whose weight in the wave function is greater than a given threshold (typically 0.01). This criterion, however, is somewhat arbitrary and cannot be used for the calculation of potential energy curves. To avoid this problem, we used the excitation degree of the CAS CSFs as the selection parameter. For example, in the case of the $\tilde{X}^1A'$ ground state of NSCl, the active space contains the HF closed shell reference configuration plus all single, double, triple... up to hexa excitations from the occupied orbitals to the empty ones. With the cc-pVQZ basis set, the resulting MRCI space contains about 5 millions of contracted CSFs. If we impose that only the closed shell HF configuration plus all the single and double excitations (which correspond to 219 CSFs among the 8029 of the full CAS) are generators of the MRCI space, the size of this space is reduced to about 1.8 million of uncontracted CSFs. When a similar procedure is applied to the case of $NSCl^+$ states (open shell HF configurations), the reduction of the MRCI space is even more drastic, and the calculations become feasible for our present computational possibilities. In the following, this type of MRCI calculations will be designed as MRCI(D).

In order to determine the equilibrium geometry of the $\tilde{X}^1A'$ ground state of NSCl, a grid of 35

points centred on the experimental geometry was generated. The resulting energies (calculated at RHF, CASSCF and MRCI levels) were then fitted by a fourth-degree polynomial, using the SURFIT program [15]. The resulting surfaces were then converted to quadratic force fields in internal and dimensionless coordinates using *l*-tensor algebra [16] as implemented in SURFIT. The program uses perturbation theory to obtain the harmonic and anharmonic wavenumbers.

A well known problem arising in the calculation of transition energies is the choice of the orbitals for the description of the initial and final states. Here, for the calculations of the electronic states of $NSCl^+$, three types of CASSCF MOs were employed: the NSCl ground state MOs, state-averaged (SA) MOs for the four lowest-lying states of $NSCl^+$ (for each irreducible representation A′ and A″) and state-optimised MOs for each ionic state.

Finally, in order to interpret the vibrational structure of the spectral bands, Franck–Condon factors calculations were carried out, using our local implementation [17,18] of the method proposed by Cederbaum and Domcke [19]. This model requires the determination of the gradient (the κ matrix) and the Hessian (the γ matrix) of the ionisation energy E_v at the neutral geometry:

$$\kappa_i = 2^{-1/2}\left(\frac{\partial E_v}{\partial Q_i}\right)_0, \quad \gamma_{ij} = \frac{1}{4}\left(\frac{\partial^2 E_v}{\partial Q_i \partial Q_j}\right)_0.$$

In the present work, the quadratic coupling matrix γ was neglected and only the κ matrix was computed (linear coupling approximation) at the CASSCF/cc-pVQZ level.

3. Experimental

3.1. Sample preparation

The trimer of thiazyl chloride $N_3S_3Cl_3$ was made using the method described by Jolly and Maguire [20]. This is a two-step synthesis. First, disulfurdichloride, S_2Cl_2, reacts with ammonium chloride, NH_4Cl producing $S_3N_2Cl_2$ which then reacts with chlorine, Cl_2, to give the solid product, $S_3N_3Cl_3$.

$$4S_2Cl_2 + 2NH_4Cl \rightarrow S_3N_2Cl_2 + 8HCl + 5S$$

$$3S_3N_2Cl_2 + 3Cl_2 \rightarrow 2N_3S_3Cl_3 + 3SCl_2$$

The preparation was carried out in small batches, using 1/10th of the quantities recommended in the original recipe. Consequently, the first reaction step was completed in about 3 h (rather than 10–12 h) and the intermediate $S_3N_2Cl_2$ was chlorinated directly. At stages when moist air had to be excluded, oxygen-free nitrogen was flowed through the system. The final batches of product were stored in air-tight sample bottles. Portions were transferred, as required, to a sample tube that was connected directly to the ionisation chamber of the photoelectron spectrometer. Rapid heating under vacuum to 70 °C released the monomer.

3.2. Photoelectron spectrometer

The HeI photoelectron spectra were recorded using an hemispherical energy analyser described elsewhere [21]. The resolution was set to 20 meV, measured as the full width at half height of the $^2P_{3/2}$ peak of the argon HeI photoelectron spectrum.

The resolution was further increased by deconvolution using a procedure described by van Cittert [22] and modified by Allen and Grimm [23]. The energy axis was calibrated with reference to HCl and N_2, present as impurities in some of the spectra, using the values given by Kimura [24]. The spectra have been corrected for the transmission of the electron optics.

4. Results and discussion

4.1. The electronic ground state $\tilde{X}^1A'$ of the neutral molecule

At the Hartree–Fock level, the electronic configuration of the $\tilde{X}^1A'$ ground state is

[core]1a′2a′3a′4a′5a′1a″6a′2a″7a′

The experimental equilibrium geometry was determined by microwave spectroscopy [1] and X-ray diffraction [2] (see Table 1). The two sets of values agree well with each other. At the theoret-

ical level, the only ab initio determination is that of Ehrhardt and Ahlrichs [25], using the coupled pair functional (CPF) method [26] but with the NSCl angle kept frozen to 117.7° (Table 1). This study emphasised the importance of polarization functions (especially g AOs) for a good description of the NSCl bond lengths.

Our own calculated geometries using the cc-pVTZ and cc-pVQZ basis sets are presented in Table 1. As expected for these methods, the RHF bond lengths are underestimated while the CASSCF ones are overestimated. In particular, the S–Cl bond length is too large at cc-pVQZ/CASSCF level by 0.07 Å. The full MRCI and MRCI(D) calculations using the cc-pVTZ basis set slightly improve the result with a S–Cl bond length around 2.2 Å, which is too large by ≈0.04 Å. Finally, the cc-pVQZ/MRCI(D) calculations give the best results, with a remaining discrepancy between theory and experiment of 0.015 Å for R_{SCl}.

The vibrational wavenumbers of NSCl have also been determined, using infrared spectroscopy in the gas phase by Müller et al. [3] and in argon matrices by Peake and Downs [27] (see Table 2). The three modes correspond, respectively, to the N–S stretching mode (ν_1), to the N–S–Cl bending mode (ν_2) and to the S–Cl stretching mode (ν_3). The calculated wavenumbers, obtained at RHF, CASSCF and MRCI(D) levels with both basis sets are given in Table 2. Several well known trends can be observed, such that the 10% overestimation of the RHF values. The harmonic wavenumbers are too high in most cases and the inclusion of anharmonicity improves the situation. The basis set effects are less important than for the geometries, the difference between the cc-pVTZ and cc-pVQZ being less than 10 cm^{-1} in most cases. Among the three modes, the bending and S–Cl stretching values are very close to the experimental ones. For these two modes, anharmonic effects seem to be weak since at all levels of theory, the differences between the ω and the ν values are negligible. The MRCI(D) results seem to give slightly poorer results, since the anharmonic values remain above the experimental ones. This tends to indicate that the restrictions of MRCI(D) method described above slightly affect the topology of the potential well around the equilibrium geometry.

4.2. The ionic states

4.2.1. Photoelectron spectrum

The HeI photoelectron spectrum is displayed in Fig. 1. We note that bands 1 and 2 are structureless with FWHM of about 0.18 and 0.46 eV, respectively. Concerning the second band, the results of the calculations described below show that it is the superposition of two displaced peaks with the same FWHM. The result of the fitting of this band by two identical Gaussian functions is displayed in Fig. 2. The energy spacing is 0.224 eV and the FWHM is 0.27 eV. Band 3 shows a vibrational progression, with a wavenumber of about 290 cm^{-1} (0.036 eV) consistent with excitation of the bending vibration ν_2, which has a wavenumber of 271.6 cm^{-1} (0.034 eV) in the ground state

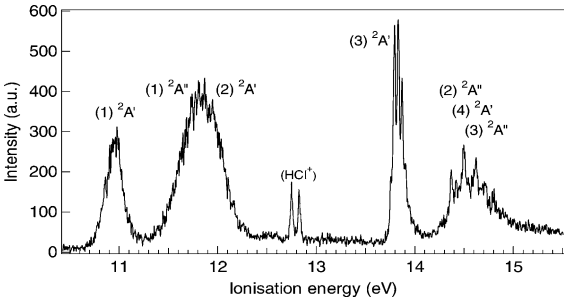

Fig. 1. The HeI photoelectron spectrum of NSCl.

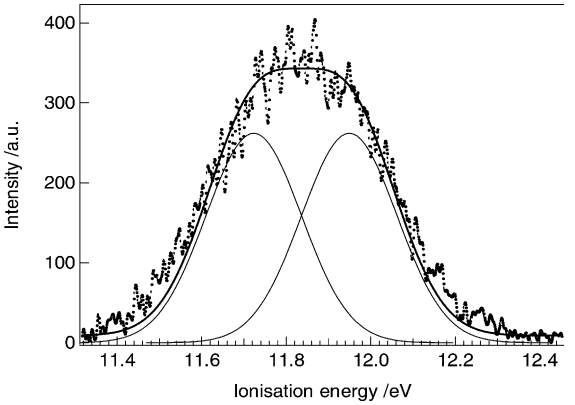

Fig. 2. Results of the fitting of the second peak of the experimental spectrum by two identical displaced Gaussians functions.

Table 3
Calculated vertical ionisation energies of NSCl (eV)

	This work							
	Neutral MOs[a]	SA MOs[a]	Optimised MOs	Exp.	Exp.[b]	Exp.[c]	HF[d]	EH[e]
$(1)^2A'$	10.670	10.346	10.362	10.953	10.96	10.95 (1)	11.27 (7a′)	11.69 (7a′)
$(1)^2A''$	11.679	11.239	11.227	11.725	11.80	11.82 (2)	12.48 (2a″)	12.89 (6a′)
$(2)^2A'$	12.075	11.237	11.153	11.949			12.71 (6a′)	13.04 (2a″)
$(3)^2A'$	14.012	13.474	13.394	13.834	13.77	13.83 (2)	15.92 (1a″)	14.33 (5a′)
$(2)^2A''$	14.587	14.349	13.958	14.499	14.46	14.49 (1)	16.19 (5a′)	15.25 (4a′)
$(4)^2A'$	14.703	14.254	14.202				17.25 (4a′)	
$(3)^2A''$	14.777	14.016	14.404					
$(4)^2A''$	16.291	14.874	15.042					

[a] MRCI(D) values obtained at the calculated MRCI(D)/cc-pVQZ equilibrium geometry of NSCl (see Table 1) and corrected of the ZPE (1035.1 cm^{-1} or 0.128 eV, Table 2).
[b] Ref. [5].
[c] Ref. [6].
[d] Koopmans MOs energies from [7].
[e] Extended Hückel calculations from [5].

neutral molecule. De Kock et al. [6] identified a similar progression in the NeI spectrum, citing a wavenumber of 250 ± 30 cm^{-1} (0.031 ± 0.04 eV). In band 4 vibrational intervals of about 1049 cm^{-1} (0.13 eV) and 403 cm^{-1} (0.05 eV) may be identified; these could relate to excitation of the two stretching vibrations v_1 and v_3 (1325 cm^{-1} or 0.164 eV and 415 cm^{-1} or 0.0514 eV, in the neutral ground state, respectively). However, as will be shown later, this band is complex and its analysis in terms of a single ionisation is simplistic.

4.2.2. Vertical ionisation energies

In Table 3, the vertical ionisation energies calculated at the cc-pVQZ/CASSCF-MRCI(D) level, using the three different types of MOs are reported, as well as the results of previous calculations, based on Koopmans' theorem [5,7]. The present experimental values have been determined in the following way: for the first band, the ionisation potential is taken as the maximum of the band. The two values given for the second band are extracted for the fit by two Gaussian functions. For the third and fourth bands, the values reported in Table 3 are those of the most intense vibrational peaks.

The comparison between the three sets of calculations and the experiment shows that the theoretical results are underestimated, in most cases by several tenths of eV. The use of the neutral MOs seems to give values closer to the experimental ones, but this is an artefact: since the NSCl MOs are not the best choice for the description of $NSCl^+$ states, the calculated energies are too high. Nevertheless, all the calculations agree to assign without ambiguity the first band to the $(1)^2A'$, the second one to the $(1)^2A''$ and $(2)^2A'$ states and the third one to the $(3)^2A'$ state. These results are in agreement with the Koopmans values [5,7], except that Allaf et al. [7] assigned the third band to a A'' state. Concerning the fourth band, one can only say that it is due to several electronic states. According to the theoretical results, there are four states in the 14–15 eV energy region corresponding to this band.

Another problem concerns the ordering and the energy splitting of the $(1)^2A''$ and $(2)^2A'$ states responsible for the second band. The three types of calculations give contradictory results: the neutral MOs give 0.4 eV, which seems too high; SA calculations give quasi-degenerate values while optimised MOs lead to $\Delta E = 0.074$ eV. Relying on this latter value, which is the closest to the splitting deduced from the fit of the experimental band (0.224 eV), the ordering of the states would be $(2)^2A'$ and $(1)^2A''$.

4.2.3. Detailed investigation of the three first bands of the photoelectron spectrum

Despite the good energy resolution used to record the experimental HeI photoelectron

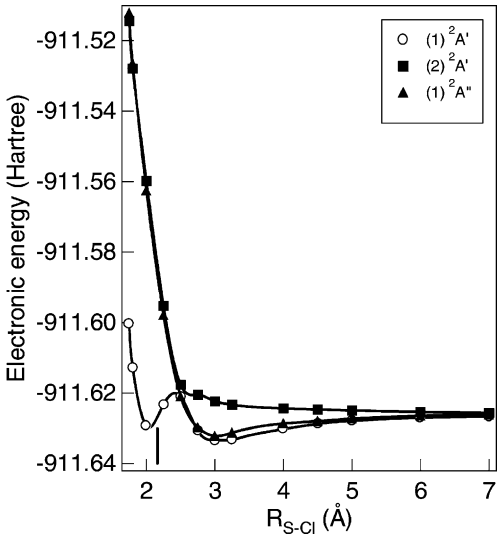

Fig. 3. Calculated potential energy curves of the lowest lying states of $NSCl^+$ (see text for details).

spectrum, no vibrational feature is observed for the two first bands of the spectrum while well resolved vibational structure is observed in the third band. In order to ascertain the reasons for such behaviour, we explored the topology of the potential energy surfaces of the lowest lying $(1)^2A'$, $(1)^2A''$ and $(3)^2A'$ states of $NSCl^+$, which correlates to the $NS^+(X^1\Sigma^+) + Cl(^2P)$ fragments (using the cc-pVTZ basis set). To do this, we optimised (at CASSCF level) the R_{NS} and $\theta_{(NSCl)}$ coordinates for different (frozen) values of R_{SCl} for the lowest lying state $(1)^2A'$ of $NSCl^+$; then, at these geometries, the SA-MRCI(D) energies of the three states were recalculated. The results of these calculations are reported in Fig. 3. In addition, a full geometry optimisation of the lowest lying states of $NSCl^+$ was performed at the CASSCF/cc-pVQZ level. A Mulliken population analysis was also carried out. The bond orders, which are not available in MOLPRO, were obtained with the HONDO package [29]. The results of these calculations are given in Table 4.

Concerning the $(1)^2A'$ state, which is responsible of the first band, the potential energy curve (Fig. 3) presents two minima, the lowest lying around 3.3 Å and the secondary one around 2.0 Å. Indeed, geometry optimisations found the equilibrium geometries indicated in the two first columns of Table 4. In the following, this secondary minimum will be denoted as (1a) to distinguish it from the lowest lying one (1b). Since (1a) takes place in the Franck–Condon zone of the neutral molecule (around 2.2 Å, vertical line in Fig. 3), one should expect the presence of vibrational features in the first band. In order to explain its absence, we have calculated the Franck–Condon factors for this state, using the force constant matrix of NSCl ($\tilde{X}^1A'$) and the κ matrix of $NSCl^+$ ($(1a)^2A'$) obtained at the cc-pVQZ/CASSCF level. The simulated band is in good agreement with the experimental one as shown in Fig. 4. In fact, this band involves excitation of both the S–Cl stretching and the bending modes, which are very close as shown in Table 2. The absence of fine structure is due to the overlapping of two vibra-

Table 4
Calculated properties (CASSCF/cc-pVQZ) of the lowest lying electronic states of $NSCl^+$

	$NSCl^+$				NSCl	NSCl[a]	NSCl[b]
	$(1a)^2A'$	$(1b)^2A'$	$(1)^2A''$	$(3)^2A'$	$\tilde{X}^1A'$	$\tilde{X}^1A'$	$\tilde{X}^1A'$
R_{NS} (Å)	1.524	1.447	1.447	1.470	1.461	1.444	1.450 ± 0.0001
R_{SCl} (Å)	2.046	3.342	3.342	2.171	2.229	2.140	2.161 ± 0.0001
θ_{NSCl} (°)	108.03	118.68	118.07	111.72	117.51	114.4	117.42 ± 0.05
Q_N	+0.01	+0.03	+0.03	+0.06	−0.27	−0.37	
Q_S	+0.82	+0.93	+0.93	+0.87	+0.63	+0.73	
Q_{Cl}	+0.17	+0.04	+0.04	+0.07	−0.36	−0.36	
σ_{NS}	1.83	2.53	2.53	1.88	2.34	2.14	
σ_{SCl}	1.02	0.01	0.01	0.89	0.72	0.60	
σ_{NCl}	0.07	0.06	0.06	0.19	0.15		

[a] HF/TZ + 2P from [4].
[b] Ref. [1].

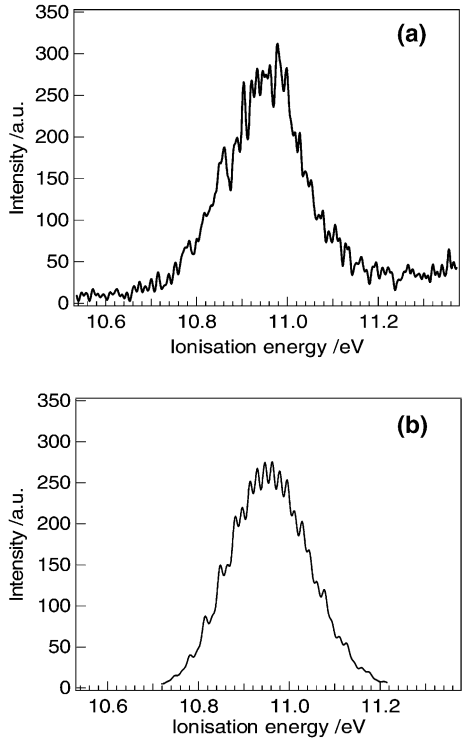

Fig. 4. First electronic band of the HeI photoelectron spectrum of NSCl. (a) Experimental curve. (b) Calculated curve (the energy maximum is set to the experimental value).

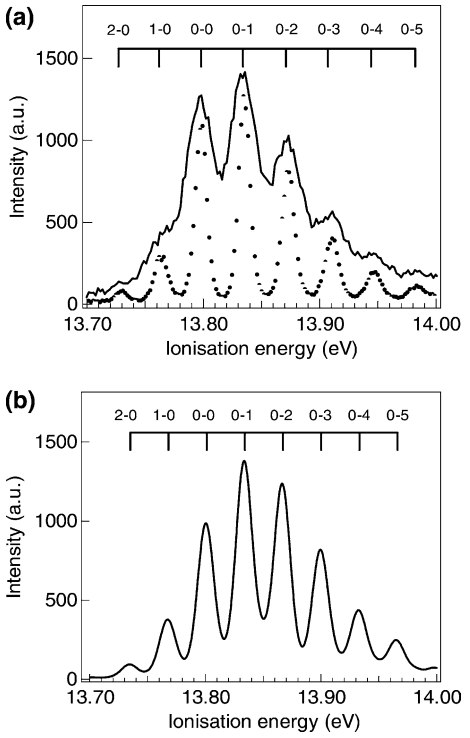

Fig. 5. Third electronic band of the HeI photoelectron spectrum of NSCl. (a) Experimental curve and (dots) deconvoluted curve (×0.4). (b) Calculated curve (the energy of the most intense peak is set to the experimental value).

tional progressions. Moreover, it should be noticed that our calculations do not take into account the tunnelling effect through the potential energy barrier occurring around 2.5 Å (Fig. 3). This should increase the width of the vibrational peaks, at least on the high energy side of the band, and contribute to the absence of fine features.

For the second band, assigned to the $(2)^2A'$ and the $(1)^2A''$ states of $NSCl^+$, inspection of Fig. 3 shows that, in the Franck–Condon zone of the neutral ground state, their potential energy curves are highly repulsive (the $(2)^2A'$ is in fact dissociative) and well above the dissociation asymptote. Furthermore, the $(2)^2A'$ and $(1)^2A''$ potential energy curves have the same slope. After the reflection principle [28], it is possible to estimate from this slope the width of the spectral bands. The resulting value (0.35 eV) is consistent with the value obtained in the fitting of the second experimental band (0.27 eV) as shown in Fig. 2. The repulsive character of potential energy curves explains the absence of vibrational structure in the spectrum for this band.

The situation is somewhat different for the third band of the photoelectron spectrum, corresponding to the $(3)^2A'$ state whose geometry and charge properties are very close to the one of the neutral ground state, as shown in Table 4. By comparison with the wavenumber values in NSCl (Table 2), we can attribute the observed vibrational features in this band of the photoelectron spectrum to ν_2, the bending vibration mode. Another indication is the fact that the main difference between the geometries of the $NSCl^+$ $(3)^2A'$ state and the neutral ground state is the $\theta_{(NSCl)}$ angle (Table 4).

In order to assign precisely the experimental peaks, we have calculated the Franck–Condon factors for this state, using the same method as for the first band. The calculated shape of this third

band is shown in Fig. 5(b) and can be compared to the experiment shown in Fig. 5(a). Despite the simplicity of the model, the overall agreement with the experimental spectrum is good, the main discrepancy being the relative intensity of the third and fifth peaks. According to these calculations, the two first peaks observed correspond to hot band type transitions from the $(0,\ v_2'' = 1, 2,\ 0)$ levels of the $\tilde{X}^1A'$ ground state of NSCl to the $(0,0,0)$ level of the $(3)^2A'$ electronic state of $NSCl^+$. All the following observed peaks correspond to transitions from the $(0,0,0)$ vibrational level of NSCl to the $(0,v_2',0)$ levels of the ionic state. This gives a value of 13.798 ± 0.002 eV for the adiabatic formation of the $(3)^2A'$ electronic state of $NSCl^+$. Moreover, the model predicts that the intensity ratio of the $(v_2'' = 1 \rightarrow v_2' = 0)$ and the $(v_2'' = 0 \rightarrow v_2' = 1)$ transition should match the Boltzmann factor $exp(-v_2/kT)$, i.e., about 0.27 in the present case. This value is in good agreement with the one (around 0.26) deduced form the experimental band shown in Fig. 5(a).

In addition to the geometries, Table 4 shows the Mulliken populations and bond orders of the lowest lying states of $NSCl^+$. For all the structures, the positive charge is located on the sulphur atom. The (1a) and $(3)^2A'$ states, whose geometries are rather close to the neutral one, the charge properties and bond orders are also similar to those of NSCl. On the other hand, the $(1b)^2A'$ and $(1)^2A''$ states of $NSCl^+$ are nearly indistinguishable. These states are very weakly bound complexes between the Cl atom and a NS^+ ion. The A'–A'' splitting is due to the removal of the electron from the in-plane and out-of-plane π orbital which constitutes the HOMO of the neutral NS molecule.

Finally, for the fourth band, one can only say that it is very difficult to perform a detailed theoretical study, as this would require the determination of the ionisation energies, the absolute electronic ionisation intensities and the vibrational wavenumbers of at least three highly excited states.

5. Conclusions

In the present paper, we have reinvestigated the HeI photoelectron spectrum of NSCl, combining a high resolution spectrum, large scale (CASSCF-MRCI) ab initio methods, and Franck–Condon factors calculations. For the three first bands of the spectrum, the theoretical results provide assignments that improve on those from previous semi-empirical calculations. Geometry optimisations of the lowest lying states of $NSCl^+$ and Franck–Condon analysis are used to explain the vibrational structure (or its absence) in the three first bands. In particular, the theoretical simulation of the vibrational progression observed in the third band reveals the presence of hot bands and leads to the conclusion that the adiabatic ionisation energy of the $(3)^2A'$ electronic state of $NSCl^+$ is 13.798 eV.

Acknowledgements

The Laboratoire de Physique des Lasers, Atomes et Molécules (PhLAM) is a "Unité Mixte de Recherche du CNRS" of France. The Centre d'Études et de Recherches Lasers et Applications (CERLA) is supported by the Ministère chargé de la Recherche, the Région Nord/Pas-de-Calais of France, and the Fonds Européen de Développement des Régions (FEDER). M.J.H.F. acknowledges the Fonds National de la Recherche Scientifique for a research position. ICW is grateful to the Fonds National de la Recherche Scientifique for funding her stay if the Liège laboratories. The authors thank the referee for very useful suggestions.

References

[1] T. Beppu, E. Hirota, Y. Morino, J. Mol. Spectrosc. 36 (1970) 386;
S. Mizumoto, J. Izumi, T. Beppu, E. Hirota, Bull. Chem. Soc. Jpn. 45 (1972) 786.
[2] W.C. Emken, K. Hedberg, J. Chem. Phys. 58 (1973) 2195.
[3] A. Müller, N. Mohan, S.J. Cyvin, N. Weinstock, O. Glemser, J. Mol. Spectrosc. 59 (1976) 161.
[4] C. Ehrhardt, R. Ahlrichs, Chem. Phys. 108 (1986) 417.
[5] D.O. Cowan, R. Gleiter, O. Glemser, E. Heilbronner, Helv. Chim. Acta 55 (1972) 2418.
[6] D.L. De Kock, M.A. Shehfeh, D.R. Lloyd, P.J. Roberts, J. Chem. Soc. Faraday II 72 (1976) 807.

[7] A.W. Allaf, G.Y. Matti, R.J. Suffolk, J.D. Watts, J. Electron Spectrosc. Rel. Phenom. 48 (1989) 411.
[8] MOLPRO (version 2000.1) is a package of ab initio programs written by H.-J. Werner and P.J. Knowles with contributions from R.D. Amos, A. Bernhardsson, A. Berning, P. Celani, D.L. Cooper, M.J.O. Deegan, A.J. Dobbyn, F. Eckert, C. Hampel, G. Hetzer, T. Korona, R. Lindh, A.W. Lloyd, S.J. McNicholas, F.R. Manby, W. Meyer, M.E. Mura, A. Nicklass, P. Palmieri, R. Pitzer, G. Rauhut, M. Schütz, H. Stoll, A.J. Stone, R. Tarroni, and T. Thorsteinsson. Available from: http://www.tc.bham.ac.uk/molpro.
[9] T.H. Dunning, J. Chem. Phys. 90 (1989) 1007.
[10] H.-J. Werner, P.J. Knowles, J. Chem. Phys. 82 (1985) 5053.
[11] P.J. Knowles, H.-J. Werner, Chem. Phys. Lett. 115 (1985) 259.
[12] H.-J. Werner, Adv. Chem. Phys. 69 (1987) 1.
[13] H.-J. Werner, P.J. Knowles, J. Chem. Phys. 89 (1988) 5803.
[14] H.-J. Werner, P.J. Knowles, Chem. Phys. Lett. 145 (1988) 514.
[15] J. Senekowitsch, Ph.D. Thesis, University of Frankfurt, 1988.
[16] A.R. Hoy, I.M. Mills, G. Strey, Mol. Phys. 24 (1972) 1265.
[17] J.-P. Flament, Ph.D. Thesis, Université de Paris-Sud, Centre d'Orsay (1981).
[18] J.-P. Dognon, C. Pouchan, A. Dargelos, J.-P. Flament, Chem. Phys. Lett. 109 (1984) 492.
[19] L.S. Cederbaum, W. Domcke, Adv. Chem. Phys. 36 (1977) 205.
[20] W.L. Jolly, K.D. Maguire, Inorg. Synth. 9 (1967) 102.
[21] J. Delwiche, P. Natalis, J. Momigny, J.E. Collin, J. Electron Spectrosc. Relat. Phenom. 1 (1972) 219.
[22] P.H. van Cittert, Z. Phys. 69 (1931) 298.
[23] J.D. Allen Jr., F.A. Grimm, Chem. Phys. Lett. 66 (1979) 72.
[24] K. Kimura, S. Katsumata, Y. Achiba, T. Yamazaki, S. Iwata, Handbook of HeI Photoelectron Spectra of Fundamental Organic Molecules, Halsted Press, New York, 1981.
[25] C. Ehrhardt, R. Ahlrichs, J. Chem. Phys. 82 (1985) 890.
[26] R. Ahlrichs, P. Scharf, C. Ehrhardt, Chem. Phys. 108 (1986) 417.
[27] S.C. Peake, A.J. Downs, J. Chem. Soc. (Dalton) (1974) 859.
[28] R. Schinke, Photodissociation Dynamics, Section 6.1, Cambridge Monographs on Atomic, Molecular and Chemical Physics 1, Cambridge University Press, 1993.
[29] M. Dupuis, F. Johnston, A. Marquez, HONDO95.3 from CHEM-Station, IBM Corporation, Neighborhood Road, Kingston, NY, 12401, USA, 1995.